

CRYSTALLIZATION KINETICS OF THE $\text{Cu}_{0.3}(\text{SSe}_{20})_{0.7}$ CHALCOGENIDE GLASS

A. A. Soliman*, M.B. El-Den
Physics Department, Faculty of Science, Ain Shams University,
Abbassia-11566, Cairo, Egypt

The crystallization kinetic parameters: the activation energy of growth, E_G , the Avrami exponent, n , and the frequency factor, k_0 for the $\text{Cu}_{0.3}(\text{SSe}_{20})_{0.7}$ chalcogenide glass has been studied by three different models: Augis-Bennett, Gao-Wang and Matusita. The non-isothermal differential scanning calorimetry (DSC) curves indicate that this glass crystallizes by a two-stage bulk crystallization process upon heating.

(Received February 28, 2007; accepted March 1, 2007)

Keywords: Cu-S-Se, Chalcogenide, Glass, crystallization

1. Introduction

The chalcogenide vitreous semiconductors (ChVS) have attracted much attention in the field of photo-induced effects since they exhibit photo-stimulated diffusion of metals (mainly Ag or Cu) into ChVS, which are applicable in a variety of microelectronics, optical memory, holography, diffractive optics and photoresistors [1-5]. These materials must be stable in the amorphous state at low temperature and have a short crystallization time [6,7]. Therefore it is very important to know the glass forming ability and chemical durability of this type of materials.

The increasing use of thermoanalytical techniques such as differential thermal analysis (DTA) or differential scanning calorimetry (DSC) has offered the promise of obtaining useful data with simple methods [8]. The utilization of the thermoanalytical techniques depends in turn on the development of methods for analyzing the experimental data. With this objective, a large number of mathematical treatments are based on the formal theory of transformation kinetics.

According to the kinetic viewpoint, when glass transform into the crystalline state it must overcome some potential barriers. It is the activation energy of crystallization which the rearranged particles have to overcome. If the potential barrier is higher, i.e. the activation energy of crystallization is larger, the nucleation and crystallization of the glass are more difficult and the particles have not enough time to rearrange when the glass melt is rapidly quenched. This is favorable for glass formation [8].

The crystallization of a glass upon heating can be performed in several ways. In calorimetric measurements, two basic methods can be used, isothermal and non-isothermal. However, the results of crystallization process can be interpreted in terms of several theoretical models [9, 10].

The present work is focused on the derivation and application of three different theoretical models used to study the crystallization kinetics of $\text{Cu}_{0.3}(\text{SSe}_{20})_{0.7}$ chalcogenide glass prepared for the first time by the melt quenching technique.

2. Theoretical analysis

The theoretical basis for the interpretation of the DSC results is provided by the formal theory of transformation kinetics. This theory describes the evolution with time, t , of the crystallized fraction χ in terms of the crystalline growth rate u :

*Corresponding author: Alaa_soliman2000@hotmail.com

$$\chi = 1 - \exp \left[-g \left(\int_{t'}^t u \, d\tau \right)^n dt' \right] = 1 - \exp(I^n) \quad (1)$$

Where g is a geometric factor which depends on the shape of the crystalline growth and n is a parameter which depends on the mechanism of transformation. It has been pointed out[1,6,7] that in non-isothermal measurements, generally due to a rapid temperature rise and big differences in the latent heats of nucleation and growth, the crystallization exotherm characterizes the growth of the crystalline phase from the amorphous matrix; nucleation is more or less calorimetrically unobservable at temperatures below the crystallization exotherm, or it takes place very rapidly and immediately after overheating of the material in the initial stages of the crystallization exotherm, which results in the deformed beginning of the measured exotherm. Therefore, In eq.(1) it is assumed that the nucleation process takes place early in the transformation and nucleation rate is zero thereafter. This process of heterogenous nucleation has been quoted as "site saturation"[11, 12]. Eq.(1) can be taken as a detailed specific case of the Johnson-Mehl-Avrami[13-15] equation:

$$\chi = 1 - \exp[-(kt)^n] \quad (2)$$

Where n is the reaction order, or Avrami index, and k the reaction-rate constant, whose temperature dependence is generally expressed by the Arrhenius equation:

$$k = k_0 \exp[-E_G/RT] \quad (3)$$

where k_0 is the frequency factor, E_G activation energy for growth, R gas constant and T absolute temperature. Differentiation of Eq.(3) with respect to t , at constant temperatures gives

$$\frac{d\chi}{dt} = nk^n t^{n-1} (1 - \chi) \quad (4)$$

where $d\chi/dt$ is the rate of crystallization at time t . In this paper, we use three different mathematical treatments based on Eq.(2) to determine the kinetics parameters, which are briefly described below.

2.1. Augis and Bennett method

In a non-isothermal DSC experiment, the temperature is changed linearly with time at a known heating rate $\alpha(=dT/dt)$, i.e.

$$T = T_0 + \alpha t \quad (5)$$

Where T_0 is the starting temperature and T is the temperature after time t . As the temperature constantly changes with time, kt is no longer a constant but varies with time in a more complicated function such as:

$$kt = u = k_0 t \exp \left[-\frac{E_G}{R(T_0 + \alpha t)} \right] \quad (6)$$

and Eq.(2) becomes

$$\chi = 1 - \exp(-u^n) \quad (7)$$

If the rate of transformation is maximum at the DSC peak, the position of the peak is given by

$$\ddot{\chi} = [\ddot{u}u - \dot{u}^2(nu^n - n + 1)]nu^{n-2}(1 - \chi) = 0 \quad (8)$$

From Eq.(6)

$$\dot{u} = u(1/t + q) \quad (9)$$

where $q = E_G \alpha / RT^2$, also for $T_0 \ll T$

$$\ddot{u} = u \left[\left(\frac{1}{t} + q \right)^2 - \frac{1}{t^2} \right] - \frac{2qu}{t} \quad (10)$$

or

$$\ddot{u} = q^2 u \quad (11)$$

substituting values of \dot{u} and \ddot{u} from Eqs.(9) and (11) into Eq.(8) gives

$$[nu^n - n + 1] = [qt/(1 + qt)]^2 \quad (12)$$

under the condition $qt \gg 1$ [or $E_G(T - T_0)/RT^2 \gg 1$] the right hand side of Eq.(12) ≈ 1 . Therefore, Eq.(12) can be written as

$$u = kt = k_0 \exp\left(-\frac{E_G}{RT_p}\right) \left(\frac{T_p - T_0}{\alpha}\right) \approx 1 \quad (13)$$

or in logarithmic form:

$$\ln\left(\frac{\alpha}{T_p - T_0}\right) = \ln k_0 - \frac{E_G}{RT_p} \quad (14)$$

where T_p is the temperature at the crystallization peak. Hence, according to Eq.(14), a plot of $\ln[\alpha/(T_p - T_0)]$ vs. $1/T_p$, measured at different heating rates, should be a straight line with slope E_G/R and intercept $\ln k_0$.

Augis and Bennet[16] reported that the crystallization mechanism could be determined from the shape factor, n of the exothermic peak represented by the following equation:

$$n = \frac{2.5}{\Delta T_{FWHM}} \cdot \frac{T_p^2}{E_G/R} \quad (15)$$

where ΔT_{FWHM} is the width of the crystallization peak at half-maximum.

2.2. Gao Yiqun and Wang method

The Gao Yiqun et al.[17] method based on the assumption that the crystallization fraction χ for the maximum rate is not changed with the heating rate. Eliminating t from Eq.(4), one obtains

$$d\chi/dt = nK(1 - \chi)[- \ln(1 - \chi)]^{(n-1)/n} \quad (16)$$

Taking the integration from the initial starting point to the maximum crystallization point rate

$$\int_0^{\chi_p} \frac{d\chi}{(1 - \chi)[- \ln(1 - \chi)]^{(n-1)/n}} = n K_0 \int_0^{t' - E_G/RT} e^{-E_G/RT} dt \quad (17)$$

The integral over χ yields

$$\int_0^{\chi_p} \frac{[-\ln(1-\chi)]^{(1-n)/n} d\chi}{(1-\chi)} = n \left[-\ln(1-\chi_p) \right]^{1/n} \quad (18)$$

Finally, Eq.(17) becomes

$$\left[-\ln(1-\chi_p) \right]^{1/n} = K_o \int_{T_o}^{T_p} e^{-E_G/RT} dt \quad (19)$$

where T_o is the starting temperature. The time integral in Eq.(19) is transformed to a temperature integral($\alpha=dT/dt$), yielding

$$\left[-\ln(1-\chi_p) \right]^{1/n} = \frac{K_o}{\alpha} \int_{T_o}^{T_p} e^{-E_G/RT} dT \quad (20)$$

The integral is further transformed by substituting $y=E_G/RT$

$$\left[-\ln(1-\chi_p) \right]^{1/n} = -\frac{E_G K_o}{\alpha R} \frac{y_p}{y_o} \int_{y_o}^{y_p} \frac{e^{-y}}{y^2} dy \quad (21)$$

This integral can be evaluated using the exponential integral function [7], if it is assumed that $T_o \ll T_p$, so that y_o can be taken as ∞ . This assumption is justifiable for any heating treatment which begins at a temperature where nucleation and crystal growth are negligible [9], i.e., below T_g for most glass-forming systems.

The exponential integral function, $E(-y)$, is represented by several approximate analytical expressions. The most convenient expression for the present problem is given by Abramovitz and Stegun[18]

$$E(-y) = \frac{-e^{-y}}{y} \left(1 - \frac{1}{y} + \frac{2}{y^2} - \frac{6}{y^3} \dots + \frac{(-1)^n n!}{y^n} \right) \quad (22)$$

When $y_o = \infty$, the integral in Eq.(21) can be expressed [3] as

$$\int_{\infty}^{y_p} \frac{e^{-y}}{y^2} dy = \frac{-e^{-y_p}}{y_p} - E_i(-y_p) \quad (23)$$

for $y_p (=E_G/RT_p) \gg 1$, the integral becomes

$$\int_{\infty}^{y_p} \frac{e^{-y}}{y^2} dy = \frac{-e^{-y_p}}{y_p} + \frac{e^{-y_p}}{y_p} \left[1 - \frac{1}{y_p} \right] = \frac{-e^{-y_p}}{y_p^2} \quad (24)$$

Substituting Eq.(24) in Eq.(21), one obtains

$$\left[-\ln(1-\chi_p) \right]^{1/n} = \frac{R k_o T_p^2}{\alpha E_G} e^{-\frac{E_G}{RT_p}} \quad (25)$$

or

$$\left[-\ln(1-\chi_p)\right]^{-1/n} = \frac{\alpha E_G}{R k_p T_p^2} \quad (26)$$

This derivation is similar to that of Gao et. Al [17]. In this work, we treated the temperature integral equation (Eq.(21)) considering the exponential integral function of order one instead of order two in Gao et al treatment. Taking the second derivative of χ with respect to t and making it zero to locate the maximum crystallization rate

$$\begin{aligned} \frac{d^2\chi}{dt^2} &= n(1-\chi)[-\ln(1-\chi)]^{(n-1)/n} \left(\frac{dk}{dt}\right)\left(\frac{dT}{dt}\right) + (nk) \frac{d\{(1-\chi)[-\ln(1-\chi)]^{(n-1)/n}\}}{d\chi} \left(\frac{d\chi}{dt}\right) = \\ &= \alpha \left(\frac{d(\ln k)}{dT}\right)\left(\frac{d\chi}{dt}\right) + (nk) \frac{d\{(1-\chi)[-\ln(1-\chi)]^{(n-1)/n}\}}{d\chi} \left(\frac{d\chi}{dt}\right) = 0 \end{aligned} \quad (27)$$

Differentiating Eq.(7) results in the following expression

$$\frac{d(\ln k)}{dT} = \frac{d(-E_G/RT)}{dT} = \frac{E_G}{RT^2} \quad (28)$$

substituting Eq.(27) into Eq.(26)

$$\left| \frac{d\{(1-\chi)[-\ln(1-\chi)]^{(n-1)/n}\}}{d\chi} \right|_p = -\frac{\alpha E_G}{n R k_p T_p^2} \quad (29)$$

where k_p and T_p are the rate and the peak temperature of crystallization at $d^2\chi/dt^2 = 0$. Differentiating the right side of Eq.(29), it becomes

$$\left| \frac{d\{(1-\chi)[-\ln(1-\chi)]^{(n-1)/n}\}}{d\chi} \right|_p = -[\ln(1-\chi_p)]^{(n-1)/n} + \frac{(n-1)}{n} [-\ln(1-\chi_p)]^{-1/n} \quad (30)$$

Substituting Eq.(25) into Eq.(30)

$$-\frac{\alpha E_G}{n k_p R T_p^2} = -\left(\frac{\alpha E_G}{k_p R T_p^2}\right)^{1-n} + \frac{n-1}{n} \left(\frac{\alpha E_G}{k_p R T_p^2}\right) \quad (31)$$

Rearranging and performing the subtraction leads to

$$\begin{aligned} \left(\frac{\alpha E_G}{k_p R T_p^2}\right)^{1-n} &= \frac{(n-1)}{n} \left(\frac{\alpha E_G}{k_p R T_p^2}\right) + \left(\frac{\alpha E_G}{n k_p R T_p^2}\right) \\ &= \frac{\alpha E_G}{k_p R T_p^2} \end{aligned} \quad (32)$$

To satisfy Eq.(32) for all values of n , it is necessary that

$$\frac{\alpha E_G}{k_p R T_p^2} = 1 \quad (33)$$

Substituting Eq.(25) into Eq.(18)

$$-\ln(1 - \chi_p) = 1 \quad (34)$$

$$\chi_p = 0.63 \quad (35)$$

inserting the expression of χ_p for χ in Eq.(11) and rearranging, one obtains an alternative form of Eq.(16) at the maximum crystallization rate point

$$\begin{aligned} \left. \frac{d\chi}{dt} \right|_p &= nk_p (1 - 0.63) \\ &= 0.37 n k_o \exp(-E_G/RT_p) \end{aligned} \quad (36)$$

Taking the logarithm of Eq.(36),

$$\ln \left(\left. \frac{d\chi}{dt} \right|_p \right) = \ln(0.37 n k_o) - \frac{E_G}{RT_p} \quad (37)$$

If the values of $(d\chi/dt)_p$ can be identified in a series of experiments of different heating rates, the plot of $\ln(d\chi/dt)_p$ versus $(1/T_p)$ should be a straight line with a slope $(-E_G/R)$. Substituting Eq.(25) into Eq.(16)

$$\left(\left. \frac{d\chi}{dt} \right|_p \right) = nk_p (1 - \chi_p) = 0.37n \left(\frac{\alpha E_G}{RT_p^2} \right) \quad (38)$$

which makes it is possible to calculate the kinetic exponent n, as

$$n = \left(\left. \frac{d\chi}{dt} \right|_p \right) RT_p^2 / 0.37 \alpha E_G \quad (39)$$

with the help of the n value and from the intercept $\ln(0.37nk_o)$, k_o can be determined.

2.3. Matusita and Sakka method

When a glass is heated at a constant heating rate, α , crystal nuclei are formed at temperatures somewhat higher than the glass temperature and grow in size at higher temperatures without any increase in number [19, 20]. For spherical crystal particles, the rate of change of the volume fraction of crystals precipitated in the glass is expressed as[20]

$$\frac{d\chi}{dt} = 4\pi r^2 (1 - \chi) N \frac{dr}{dt} \quad (40)$$

where N is the number of nuclei formed per unit volume in the temperature range from room temperature, T_r , to a certain temperature, T. For quenching glasses, N is inversely proportional to the heating rate, α and independent of α for glasses which heated for a sufficiently long time at the temperature of maximum nucleation rate. The radius, r, of a crystal particle is expressed as

$$r = \int_0^t U(T) dt = \frac{U_0}{\alpha} \int_{T_r}^T \exp(-E_G/RT) dT = \frac{C}{\alpha} \exp(-1.052 \frac{E_G}{RT}) \quad (41)$$

where R is the universal gas constant, E_G is the activation energy for crystal growth, $C = (\frac{RT^2}{E_G}) U_0$ and the rate of crystal growth, U, is expressed as[21]

$$U = U_0 \exp(-E_G/RT) \quad (42)$$

Integration of Eq.(40) and substituting the value of r from Eq.(41), for a quenched glass containing no nuclei, we have for the general case

$$-\ln(1-\chi) = K_1 \alpha^{-n} \exp(-1.052 m \frac{E_G}{RT}) \quad (43)$$

Similarly, the variation of crystal volume fraction is derived as

$$\frac{d\chi}{dt} = K_2 (1-\chi) \alpha^{-(1-n)} \exp(-1.052 m \frac{E_G}{RT}) \quad (44)$$

Here K_1 and K_2 are constants, $n=m+1$ for a quenched glass containing no nuclei and $n=m$ for a glass containing a sufficiently large number of nuclei.

In order to obtain the n-value, Eq.(43) rewritten as

$$\ln[-\ln(1-\chi)] = -n \ln \alpha - \frac{1.052 m E_G}{RT} + \text{constant} \quad (45)$$

A plot of $\ln[-\ln(1-\chi)]$ versus $\ln \alpha$ at a fixed temperature gives a straight line whose slope gives the value of n. Knowing the crystallization mechanism, the activation energy for crystallization, E_G , can be obtained by plotting a graph of $\ln[-\ln(1-\chi)]$ versus $1000/T$. The plot should be a straight line whose slope gives mE_G .

3. Experimental procedure

The $\text{Cu}_{0.3}(\text{SSe}_{20})_{0.7}$ chalcogenide glass has been prepared by the quenching technique[3,18]. Differential Scanning calorimetry (DSC) was performed on a Shimadzu DSC-50 instrument with selected heating rates 2-30 K/min in the range 300-873 K. The temperature precision of the equipment is ± 0.1 K. The samples with masses of ≈ 15 mg encapsulated in conventional platinum sample pans in an atmosphere of dry nitrogen at a flow of 30 ml/min. The instrument was calibrated prior to measurement by using high purity metal standards (In, Pb, and Zn) with known latent heat. The values of the glass transition temperature (T_g), the onset temperature of crystallization (T_c), the peak temperature of crystallization (T_p) and the melting temperature (T_m) were determined by using the microprocessor of the apparatus.

4. Results and discussion

A representative DSC curves of crystallization of the $\text{Cu}_{0.3}(\text{SSe}_{20})_{0.7}$ chalcogenide glass at various heating rates of 2, 5, 10, 15, 20, 25 and 30 K/min are shown in Fig. 1. Fig.1 indicates that the glass transition temperature of the present glass is 309.4 ~ 321.6 K, and the crystallization reaction begins to occur from 342 ~ 361.9 K for the first peak and 375.3 ~ 393.8 K for the second peak, and the temperature at maximum precipitation are 349.8 ~ 374.3 K and 381.9 ~ 399.7 K for the first and

second peaks, respectively. Values of the characteristic temperatures T_g , T_c , T_p and T_m for the investigated $\text{Cu}_{0.3}(\text{SSe}_{20})_{0.7}$ glass are listed in Table 1 as a function of the heating rates. The Table reveals that these values are shifted to higher temperatures with increasing heating rate. Another interesting feature is that the intensity (i.e. peak height) and the area under the DSC traces increase with increasing heating rate. A similar observations have also been obtained by others [23- 28].

Table 1. Characteristic temperatures for the crystallization of the $\text{Cu}_{0.3}(\text{SSe}_{20})_{0.7}$ chalcogenide glass.

| | Heating rate α (K/min) | | | | | | |
|--------------|-------------------------------|-------|-------|-------|-------|-------|-------|
| | 2 | 5 | 10 | 15 | 20 | 25 | 30 |
| T_g (K) | 309.4 | 313.4 | 316.5 | 318.6 | 319.7 | 320.8 | 321.6 |
| T_{c1} (K) | 342.0 | 348.1 | 352.9 | 356.6 | 359.1 | 360.3 | 361.9 |
| T_{c2} (K) | 375.3 | 380.5 | 385.6 | 388.8 | 390.9 | 392.3 | 393.8 |
| T_{p1} (K) | 349.8 | 356.7 | 362.5 | 357.7 | 370.9 | 371.7 | 374.3 |
| T_{p2} (K) | 381.9 | 386.8 | 391.9 | 395.4 | 397.2 | 398.6 | 399.7 |

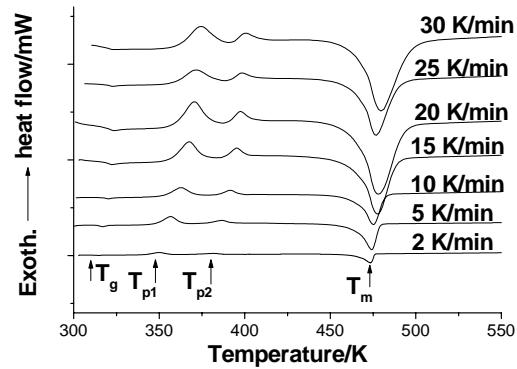


Fig.1. DSC traces for the as-prepared $\text{Cu}_{0.3}(\text{SSe}_{20})_{0.7}$ chalcogenide glass at different heating rates.

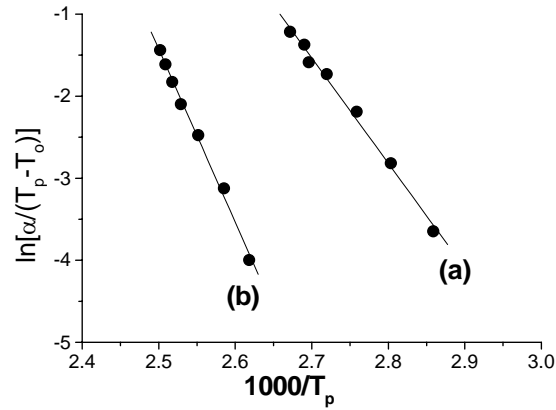


Fig.2. Plots of $\ln[\alpha/(T_p-T_o)]$ versus $1000/T_p$ and straight regression lines for : (a) the first peak and (b) the second peak of the $\text{Cu}_{0.3}(\text{SSe}_{20})_{0.7}$ chalcogenide glass.

It is reasonable to consider that the crystallization process enthalpy is directly proportional to the area of the exothermic reaction peak in the DSC curve shown in Fig.1, and the volume fraction crystallized is directly proportional to the enthalpy. So the volume fraction crystallized at a certain time t (or Temperature) can be written in the following form:

$$\chi = \frac{A_T}{A} \quad (46)$$

where A is the total area of the exothermic peak and A_T is the area under the exothermic peak at any temperature T . A plot of $\ln[\alpha/(T_p-T_0)]$ versus $1000/T_p$, shown in Fig. 2, was found to be a straight line in accordance of Eq.(14) for the first and second peaks . The width of crystallization peaks at half-maximum ΔT_{FWHM} for various heating rates for the two exothermic peaks are given in Table 2. The values of the activation energy of growth E_G and the frequency factor k_0 were calculated by least-square fitting of the data for $\ln[\alpha/(T_p-T_0)]$ versus $1000/T_p$ to Eq.(14) are to be 106.6 kJ/mol, $2.3 \times 10^{14} \text{ s}^{-1}$ and 175.5 kJ/mol, $1.9 \times 10^{22} \text{ s}^{-1}$ for the first and second peaks, respectively. Values of the Avrami exponent, n , were computed from Eq.(15) and are also listed in Table 2.

Table 2. ΔT_{FWHM} and Avrami exponent, n , for various heating rates for the $\text{Cu}_{0.3}(\text{SSe}_{20})_{0.7}$ chalcogenide glass.

| Heating rate (K/min) | First peak | | Second peak | |
|-------------------------|-------------------|------|-------------------|------|
| | ΔT_{FWHM} | n | ΔT_{FWHM} | n |
| 2 | 7.15 | 3.33 | 7.12 | 2.42 |
| 5 | 7.78 | 3.18 | 6.17 | 2.87 |
| 10 | 9.13 | 2.80 | 6.20 | 2.93 |
| 15 | 9.56 | 2.75 | 6.32 | 2.92 |
| 20 | 10.02 | 2.67 | 6.92 | 2.69 |
| 25 | 12.18 | 2.21 | 7.33 | 2.56 |
| 30 | 12.24 | 2.23 | 8.04 | 2.35 |

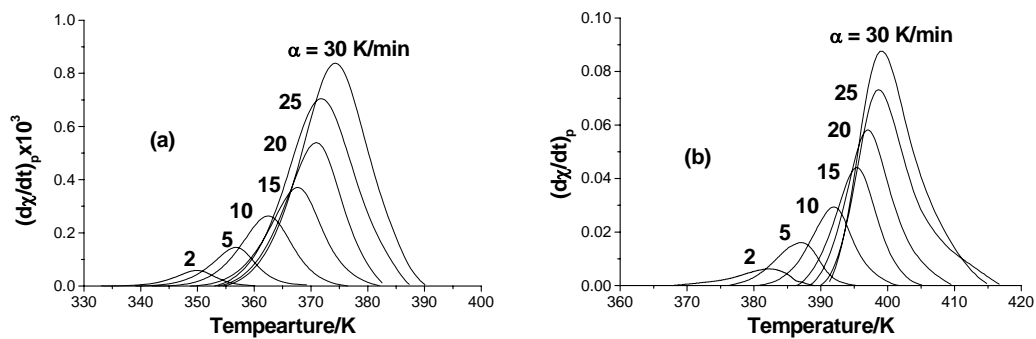


Fig. 3. Crystallization rate versus temperature of the exothermal peaks at different heating rates for : (a) the first peak and (b) the second peak of the $\text{Cu}_{0.3}(\text{SSe}_{20})_{0.7}$ chalcogenide glass.

Fig. 3. shows the exothermic curves for the first and second peaks of crystallization of $\text{Cu}_{0.3}(\text{SSe}_{20})_{0.7}$ Chalcogenide glass in DSC at heating rates of 2, 5, 10, 15, 20, 25 and 30 K/min, respectively. The height of the crystallization peak increases by the same factor as the heating rates does. Fig.4 shows the plot of $\ln(d\chi/dt)_p$ versus $1000/T_p$ for the two peaks. From the slopes of the straight lines we obtain the activation energies to be 115.62 kJ/mol and 179.58 kJ/mol for the first and second peaks, respectively. The values of the maximum crystallization rate $(d\chi/dt)_p$, the Avrami exponent, n , computed from Eq. (39) , and the values of k_0 computed from Eqs.(33) and (3) at

different heating rates for the two crystallization peaks of the investigated glass are summarized in Table 3. Although there is a certain degree of deviation in the values of n , the overall pattern is sufficiently good to conclude that the Avrami exponent, n , is independent of the heating rate. The average values of n for the first and second peaks come out to be 4 and 3, which indicate three and two dimensional growth with bulk crystallization for the first peak and second peak, respectively.

Table 3. Maximum crystallization rate $(d\chi/dt)_p$, Avrami exponent, n and the frequency factor k_o for the two crystallization peaks of the $\text{Cu}_{0.3}(\text{SSe}_{20})_{0.7}$ chalcogenide glass.

| Heating rates (K/min) | First peak | | | Second peak | | |
|--------------------------|----------------|------|-----------------------|----------------|------|-----------------------|
| | $(d\chi/dt)_p$ | n | $k_o(1/s)$ | $(d\chi/dt)_p$ | n | $k_o(1/s)$ |
| 2 | 0.00057 | 4.08 | 6.97×10^{14} | 0.00062 | 3.41 | 1.80×10^{22} |
| 5 | 0.01455 | 4.30 | 7.80×10^{14} | 0.01607 | 3.61 | 2.15×10^{22} |
| 10 | 0.02638 | 4.04 | 8.06×10^{14} | 0.02938 | 3.38 | 2.02×10^{22} |
| 15 | 0.03708 | 3.89 | 6.83×10^{14} | 0.04411 | 3.45 | 1.83×10^{22} |
| 20 | 0.05397 | 4.32 | 6.46×10^{14} | 0.05819 | 3.44 | 1.89×10^{22} |
| 25 | 0.07048 | 4.54 | 7.42×10^{14} | 0.07302 | 3.49 | 1.94×10^{22} |
| 30 | 0.08385 | 4.56 | 6.77×10^{14} | 0.08658 | 3.46 | 1.99×10^{22} |

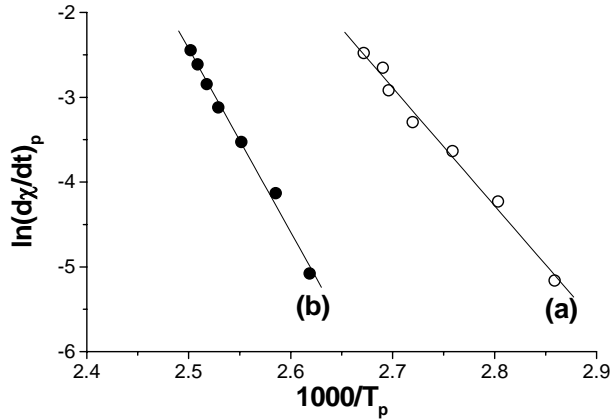


Fig.4. The maximum crystallization rate $\ln(d\chi/dt)_p$ versus the crystallization peak temperature for: (a) the first peak and (b) the second peak of the $\text{Cu}_{0.3}(\text{SSe}_{20})_{0.7}$ chalcogenide glass.

Matusita et al. Eq.(45) has been used to obtain Avrami exponent, n and the dimensionality of growth, m . A plot $\ln[-\ln(1-\chi)]$ is plotted against $\ln\alpha$ at a fixed temperature. Fig.5 shows such a plot for the two peaks of the $\text{Cu}_{0.3}(\text{SSe}_{20})_{0.7}$ chalcogenide glass at three different temperatures namely, 300, 305 and 310 K. The value of n has been evaluated from the slopes of the straight lines fit of these relations, and an average value of n was calculated to be 4.69 and 3.28 for the first and second crystallization peaks, respectively. For $\text{Cu}_{0.3}(\text{SSe}_{20})_{0.7}$ chalcogenide glass, no specific heat treatment was performed prior to the DSC scans to nucleate the sample. Therefore, n is considered to be equal to $(m+1)$ for the glass. The calculated values of n are not an integer, which means that the crystallization process of $\text{Cu}_{0.3}(\text{SSe}_{20})_{0.7}$ chalcogenide glass occurs with different mechanisms and the predominant one is the process in which $n = 4$ for first peak and $n=3$ for the second peak [29, 30]. Therefore, the value of the corresponding m is equal to 3 for first peak and $m=2$ for the second one. Therefore it is somewhat reasonable to suggest that the $\text{Cu}_{0.3}(\text{SSe}_{20})_{0.7}$ crystallization process can be carried out by a bulk crystallization in three and two dimensions for the first peak and second peak, respectively.

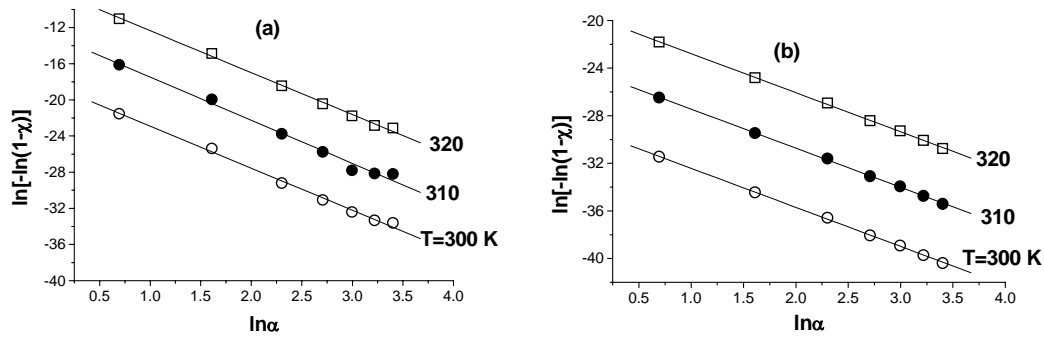


Fig.5. Plot of $\ln[-\ln(1-\chi)]$ versus $\ln\alpha$ at three different temperatures for (a) first peak and (b) second peak for $\text{Cu}_{0.3}(\text{SSe}_{20})_{0.7}$ chalcogenide glass.

To determine mE_c at different heating rates, using the Matusita and Sakka Eq.(45), a graph of $\ln[-\ln(1-\chi)]$ versus $1000/T$ for the two crystallization peaks are plotted as shown in Fig.6. The plots are found to be linear over most of the selected temperature range. Here, the analysis is restricted to the initial linear region which extends over a large temperature range [30].

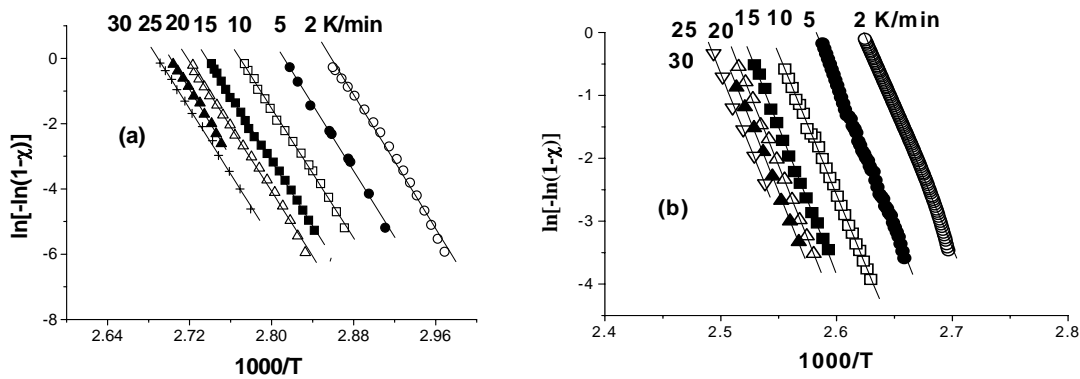


Fig.6. Plot of $\ln[-\ln(1-\chi)]$ versus $1000/T$ at three different temperatures for (a) first peak and (b) second peak for $\text{Cu}_{0.3}(\text{SSe}_{20})_{0.7}$ chalcogenide glass.

The values of mE_c at different heating rates can be obtained from the slopes of Fig. 6 and seemed to be independent of the heating rate. Therefore, an average of mE_c were calculated by considering all the heating rates. The obtained mE_c values are 398.48 KJ/mol and 365.58 KJ/mol for the first and second crystallization peaks, respectively.

In the Matusita et al. model, apart from constant heating rate, the remaining constant in Eq.(45) is equal to $\ln\{4\pi N_0(E_G U_0/R)^3/3\}$ and depending upon the growth rate, U_0 and the number of nuclei per unit volume, N_0 , the gas constant R together with the Activation energy of growth, E_G . The only unknown quantity ($U_0^3 N_0$) can be found from the intercepts straight lines ($\ln[-\ln(1-\chi)]$ versus $1000/T$) and with the help of the other known parameters such as E_G , R , n and α . The value $U_0^3 N_0$ is computed for each heating rate[31] for the two peaks of the investigated $\text{Cu}_{0.3}(\text{SSe}_{20})_{0.7}$ chalcogenide glass. With some conditions, the quantity $U_0^3 N_0$ gives the idea about the frequency factor k_0 . The reaction rate, k^n , is proportional to the quantity $I_v U^m$ (here I_v is the nucleation rate, U is the crystal growth rate and n and m have their usual parameters) with the condition that all these three parameters (k , I_v and U) have Arrhenian temperature dependence in the temperature range of crystallization peak,

having k_0 as the maximum value [9]. By substituting the value of n and m computed through the plot of $\ln\alpha$ versus $\ln[-\ln(1-\chi)]$, the order of magnitude of the frequency factor k_0 can be estimated. These values of k_0 are also given in Table 4. Further, the constant $\ln(0.37nk_0)$ appearing in the Gao-Wang model also provides direct information about the frequency factor k_0 . The computed values of the intercepts and frequency factor k_0 are also listed in Table 4.

Table 4. Kinetic parameters determined by the three methods.

| Method | First peak | | | Second peak | | |
|--------------------|-------------------|-------------------|--|-------------------|-------------------|--|
| | E_G (kJ/mol) | n | k_0 (1/s) | E_G (kJ/mol) | n | k_0 (1/s) |
| Augis and Bennett | 106.63 | 2.74 ^a | 2.36×10^{14} | 175.51 | 2.67 ^a | 1.99×10^{22} |
| Gao Yiqun and Wang | 115.62 | 4.25 ^b | 7.18×10^{14b} 7.17×10^{14c} | 179.58 | 3.45 ^b | 1.94×10^{22b} 1.95×10^{22c} |
| Matusita and Sakka | 132.83 | 4.68 | 1.16×10^{13} | 182.79 | 3.28 | 2.17×10^{27} |

^a average value calculated from Table 2.

^b average value calculated from Table 3.

^c computed from the intercept $\ln(0.37 nk_0)$.

Table 4 summarizes the values of E_G , n and k_0 obtained through the above three methods. From Table 4 it can be seen that the results from the three methods show certain differences. As to the activation energy, E_G , the values from the three methods may be considered identical for the two crystallization peak. The differences in parameter n are greater between the Augis and Bennett method with the other two methods for the two crystallization peaks. There are consistent with the n -values obtained from Gao Yiqun et al. and Matusita et al methods (see Table 4). Also, it can be seen in Table 4 that the order values of k_0 obtained from Matusita et al model differ from the other two models. This differences may be attributed to different assumptions lying in their formulations, which have already been discussed above.

5. Conclusion

The crystallization behavior of $\text{Cu}_{0.3}(\text{SSe}_{20})_{0.7}$ chalcogenide glass was studied using non-isothermal analysis method. The DSC results indicate that the glass transition temperature of the investigated glass is 309.4 ~ 321.6 K, the crystallization reactions begin to occur from 342 ~ 361.9 K and 375.3 ~ 393.8 K, and the temperatures of maximum precipitation are 349.8 ~ 374.3 K and 381.9 ~ 399.7 K. The crystallization kinetic parameters were investigated using three mathematical treatment methods. The constants appearing in the different models provide information about the frequency factor k_0 .

References

- [1] E. Illekova, J. Non-Cryst. Solids **68**, 153 (1984).
- [2] A. K. Singh, P. Kumar, K. Singh, N. S. Saxena, Chalcogenide Lett. **4**, 17 (2007).
- [3] D. I. Bletskan, Chalcogenide Lett. **3**, 81 (2006).
- [4] Ishu, S. K. Tripathi, P. B. Barman, Chalcogenide Lett. **3**, 121 (2006).
- [5] D. Lezal, J. Pedlikovo, J. Zavadil, Chalcogenide Lett. **1**, 11 (2004).
- [6] A.A. Soliman, S. Al-Heniti, A. Al-Hajry, M. Al-Assiri, G. Al-Barakati, Thermochim. Acta, **413**, 57 (2004).
- [7] A. A. Soliman, Thermochim. Acta, **423**, 71 (2004).
- [8] D.Dakui, M A Fuding, Y. U. Zhengxie, Z. Meixin, J. Non-Cryst. Solids **112**, 238 (1989).

- [9] H. Yinnon, D.R. Uhlmann, *J. Non-Cryst. Solids*, **54**, 253 (1983).
- [10] D. W. Handerson, *J. Non-Cryst. Solids*, **30**, 301 (1979).
- [11] J. W. Cahn, *Acta Metall.* **4**, 449 (1956).
- [12] J. Vázquez, C. Wagner, P. Villares, R. Jiménez-Garay, *J. Non-Cryst. Solids*, **235-237**, 548 (1998).
- [13] W.A. Johnson, K.E. Mehl, *Trans. Amr. Inst. Min. Met. Eng.* **195**, 416 (1939).
- [14] M. Avrami, *J. Chem. Phys.* **7**, 103 (1939).
- [15] M. Avrami, *J. Chem. Phys.* **8**, 212 (1940).
- [16] J.A. Augis and J.E. Bennet, *J. Therm. Anal.* **13**, 283 (1978).
- [17] Y. Q. Gao and W. Wang, *J. Non-Cryst. Solids* **81**, 129 (1986).
- [18] M. Abramowitz and I.E. Stegun, *Handbook of Mathematical Functions*, Dover, New York, 1972 .
- [19] H.J. Borchardt and F. Daniels, *J. Am. Chem. Soc.* **79**, 41 (1957).
- [20] K. Matusita and S. Sakka, *J. Non-Cryst. Solids* **38 & 39**, 741 (1980).
- [21] D. Turnbull and M.H. Cohen, " Modern Aspects of the Vitreous State", edited by J.D. Mackenzie, Butterworth, London, 1960, p.38-62.
- [22] A.A. Soliman, *Thermochim. Acta*, **435**, 129 (2005).
- [23] N.P. Bansal, R.H. Doremus, A.J. Bruce and C.T. Moynhan, *J. Amer. Ceram.Soc.* **66**, 233 (1983).
- [24] P. Wei, Li. Rongti, *Mater. Sci. Eng.* **A271**, 298 (1999).
- [25] H. Koralay, F. Yakuphanoglu, S. Cavdar, A. Günen, E. Aksu, *Physica B* **355**, 64 (2005).
- [26] A.H. Moharran, A.A. Abu-sehly, M. Abu El-Oyoun and A.S. Soltan, *Physica B* **324**, 344 (2002).
- [27] N. Afify, *Physica B* **179**, 48 (1992).
- [28] A.A. Othman, K. Tahon, M. A. Osman, *Physica B* **311**, 356 (2002).
- [29] J. Colemenero, J. M. Barandiaran, *J. Non-Cryst. Solids* **30**, 263 (1978).
- [30] A. Morotta, S. Saiello, A. Buri, *J. Non-Cryst. Solids*, **57**, 473 (1983).
- [31] Rohit Jain, N.Saxena, D. Bhandari, S. K. Sharma, K. V. R. Rao, *Physica B* **301**, 341 (2001).